CIMAC CONGRESS 25
ZURICH, MAY 19 – 23, 2025

2025 | 476

A device for accurate dynamic air flow control in a hydrogen internal combustion engine

Controls, Automation, Measurement, Monitoring & Predictive Maintenance

Georgios Bikas, Technische Hochschule Nürnberg - Fakultät Maschinenbau

Orpheas Bikas, TU Delft
Fabian Großmann, Technische Hochschule Nürnberg - Fakultät Maschinenbau
Jonas Oswald, Technische Hochschule Nürnberg - Fakultät Maschinenbau
Marius Jochem, Technische Hochschule Nürnberg - Fakultät Maschinenbau

DOI: https://doi.org/10.5281/zenodo.15193413

ABSTRACT

Over the last decade, the prevailing demand for renewable energy sources initiated the electrification of the transportation sector, with the development of H2 engines and fuel cell powertrains increasingly gaining momentum alongside battery electric vehicles. One of the essential tasks to optimize the overall efficiency of these drives is to precisely, dynamically and frictionless meter the reacting gases into the conversion chambers. In this paper, we propose a novel dosing system, focusing on gases (air), that is based on the principle of a variable Venturi nozzle, which incorporates a device for rapid variation of the effective flow cross-sectional area (EA) with negligible pressure losses. Each EA corresponds to a demanded load or mass flow and thus enables a dynamic control of the stoichiometry (l) of the machine. Our patented technology mainly consists of two surfaces perpendicular to the flow direction where one is fixed in space and the other one is moving at high frequency (> 20 Hz) towards or against the flow direction. Firstly, the underlying design philosophy and the details of the first prototype are presented, followed by an extensive description of the test bench setup, including data acquisition system. This is succeeded by a thorough analysis of the high-frequency data to extract flow characteristics and turbulence parameters. Subsequently, the transient performance of the Venturi system is experimentally compared with that of a throttle body. Finally, the capability of the Venturi system to precisely control the cycle-resolved air-fuel ratio of a hydrogen engine is demonstrated through transient simulation results based on a class B car operating under the FTP-75 driving cycle.

1 INTRODUCTION

In addition to electrification, internal combustion engines (ICEs) still offer potential for improvement, with the development of e-fuels and fuel cells gaining increasing attention.

A common challenge faced by all these technologies - e-fuel-powered ICEs, fuel cells, and hydrogen ICEs (H2-ICEs) - is the need to dynamically and accurately meter reaction gases with minimal losses.

Currently, ICEs rely on three main components to meter and control the airflow into the engine: an air mass flow sensor (MAF), a throttle body, and an oxygen sensor (λ-probe) located in the exhaust. Fresh air flows through the MAF, which provides feedback to the engine control unit (ECU). The control unit then adjusts the throttle body angle to achieve the desired airflow setpoint. Feedback information is provided by the λ-sensor, which is used to calculate the error between the desired (λ-setpoint) and the actual λ-value. The minimization of this error is subject of the control algorithms and the corresponding corrective actions managed by the ECU.

Although this approach is straightforward, it introduces significant pressure losses, especially at lower loads, due to the non-aerodynamic restriction of airflow at the throttle. Additionally, the throttled airflow lacks recovery downstream of the throttle point, resulting in turbulence that complicates real-time mass flow estimation. The system's performance is further hindered by the mass air flow sensor's lag, which delays throttle angle adjustments, and by the nonlinear behavior of the throttle itself, leading to unsynchronized responses. Consequently, the system relies heavily on static calibrations, which are only effective under steady-state conditions. During dynamic situations, such as rapid changes in engine load or speed, these limitations can result in significant deviations in air mass flow control. These inaccuracies result in substantial fluctuations in lambda values, as documented in the literature [1], ultimately causing significant spikes in NOx emissions.

The proposed device addresses these challenges by introducing an advanced dosing system tailored for internal combustion engines powered by any liquid or gaseous fuel. This system aims to enhance precision, improve dynamic response, and minimize pressure losses in reactant flows. It dynamically adjusts the effective flow cross-section at frequencies up to 25 Hz - significantly outperforming the traditional throttle body, which operates at a maximum frequency of 3 Hz - all while maintaining negligible flow losses. The system's performance is being validated through flow bench tests utilizing high-resolution aerodynamic probes capable of capturing flow velocities up to 30 kHz. These probes enable real-time and precise measurements, allowing for the experimental evaluation of the system's performance. They are detailed in [2] and have been employed in this work to resolve airflow changes during rapid transitions. Proven to be an essential tool in the development process, they significantly enhance the dosing system's optimization towards higher responsiveness and accuracy. The high-frequency data gathered from these probes will be analyzed in a later section. The paper is structured as follows: it begins with an introduction to the proposed solution and its underlying design philosophy. Next, details of the first prototype are presented, followed by an extensive description of the test bench setup, including data acquisition system. This is succeeded by a thorough analysis of the high-frequency data to extract flow characteristics and turbulence parameters. Subsequently, the transient performance of the Venturi system is experimentally compared to that of a throttle body. Finally, the capability of the Venturi system to precisely control the cycle-resolved air-fuel ratio of a hydrogen engine is demonstrated through transient simulation results based on a class B car operating under the FTP-75 driving cycle.

2 PROPOSED SOLUTION

The architecture of the proposed dosing system, referred to as a Venturi system, comprises a stationary housing and a movable component driven by an actuator (see Figure 1). By adjusting the position of the movable component, the system can modulate the width of the vena contracta (the throat area) and, consequently, the effective flow cross-section area, allowing for precise regulation of air mass flow.

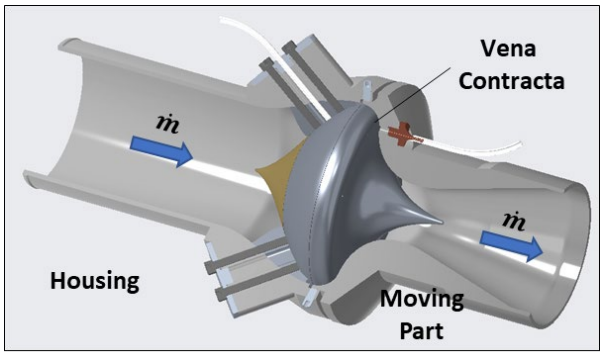

Figure 1. 3D CAD model of a design of the variable Venturi nozzle with a variable cross-sectional area and the vertical vena contracta

Due to the optimized geometry of the Venturi nozzle, pressure losses can be minimized during the throttling process, enhancing the system's efficiency. In combination with the high-frequency actuator, the desired mass flow can be set many times more dynamically than with a butterfly valve, especially in the transient range, thus reducing environmentally harmful emissions. In addition, the mass flow can be determined using advanced position sensor, eliminating the need for the expensive MAF sensor.

There are numerous scientific papers available that deal with the basic principle of the Venturi nozzle and its advantages. The applications include the mixing of air and gases [3], [4], [5], ejector refrigeration [6], [7] and span among many other technological areas. There are also international patents [8], [9] including an elastic variable Venturi nozzle for flow regulations in ICEs [10]. Additionally, Venturi nozzles have been used for fuel injectors for many years, which enables high-precision metering (deviation in the sub-mg area). However, the actual implementation of an injector principle can only be adopted to a limited extent for our purpose, as an injector always moves towards an end position (completely open - completely closed) and is not able to control at continuously variable positions.

The current study, conducted by Technische Hochschule Nuremberg (THN) and partly funded by the Bavarian state and partly by the DFG, demonstrates the feasibility of adapting the basic Venturi principle to a system with a continuously variable and adjustable cross-section (European patent [11]). The previous work combined analytical calculations, detailed flow simulations, and finite element method analysis to develop an efficient nozzle design with an integrated actuator unit. To validate the design, the THN flow bench was used for real-world performance testing.

3 DESIGN GUIDELINES AND PROTOTYPE

To ensure the optimal design of the Venturi nozzle, a multi-step approach has been employed, combining a preliminary design phase, optimization through computational fluid dynamics (CFD) simulations, and final validation via flow bench testing. The nozzle design is based on the Venturi principle, which is expected to significantly improve the system's efficiency. According to this principle, the Venturi is created by combining the shape of a convergent nozzle (flow inlet) with the geometry of a divergent diffuser (flow outlet). In this design, the smallest cross-section, known as the vena contracta, is located between the nozzle and diffuser sections (see the top image of Figure 2). The key advantage of the Venturi principle is that pressure losses caused by flow acceleration in the nozzle can be recovered during deceleration in the diffuser segment, allowing for highly efficient air mass flow control through a linear adjustment of the distance s^* (see the middle image of Figure 2).

Regarding the geometry, several key features must be met to achieve optimal pressure recovery [12]:

- The nozzle angle should not exceed 20° to ensure stable flow acceleration with high flow velocity.
- The diffuser angle should be less than 10° to prevent flow separation (stall) and maintain efficient pressure recovery.
- The contour must be smooth and continuous along the entire length of the Venturi.

To develop the variable Venturi nozzle, a static, tube-like Venturi nozzle will be initially created based on these design criteria (see the top image of Figure 2). In the first step, the required area of the vena contracta, A^* , can be determined by equation (1) using the mass flow rate $\dot{m}$, the flow velocity u^* and the air density ρ^* as defined by the operating conditions.

$$A^* = \frac{\dot{m}}{\rho^* * u^*} \tag{1}$$

By combining the area of the vena contracta A^* with an estimation of the velocity profile $M(x)$ along the flow path x the contour of the Venturi $A(x)$ can be calculated using equation (2).

$$\left(\frac{A(x)}{A^*}\right)^2 = \frac{1}{M(x)^2} * \left[\frac{2}{\kappa+1} * \left(1 + \frac{\kappa-1}{2} * M(x)^2\right)\right]^{\frac{\kappa+1}{\kappa-1}} \tag{2}$$

$$, \ with\ \kappa = 1.4$$

In the next step, the tube-like Venturi will be mapped onto a reshaped flow path, creating a design that includes two distinct curves: one for the outer housing and one for the inner part of the variable Venturi (see the middle image of Figure 2). The inner part will be further divided into a stationary segment, which will later be connected to the housing, and a movable part, driven by the actuator. It is important to emphasize that defining the shape of the flow path is a crucial step in the design process. The geometry of the variable Venturi not only affects the system's efficiency but also the requirements for the actuator (such as total displacement, dynamics, precision, and driving force). Furthermore, as previously mentioned, although Venturi nozzles have been utilized in fuel injectors, the injector principle cannot be directly applied in this context. Implementing it would lead

to a shift in the position of the vena contracta during the opening or closing phases (see the bottom image of Figure 2).

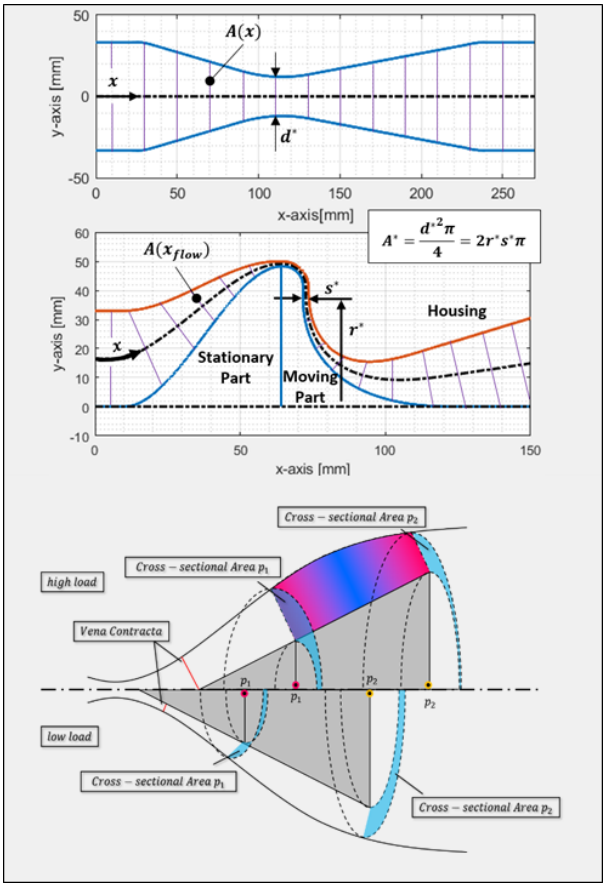

Figure 2. Guidelines for preliminary variable Venturi design. Top: Tube-like-shaped Venturi contour. Middle: Projection of the tube-like-shaped geometry along the flow path, creating the contour of the variable Venturi. Bottom: Displacement of the vena contracta during opening and/or closing by adopting the injector type principle

Therefore, when designing the flow path, the following specifications must be considered:

- Rapid changes in the direction of airflow result in pressure losses. As such, flow guidance with large radii and smooth cross-sectional transitions is beneficial to reduce these losses.
- The gradient of the inner and outer contours can cause a shift in the position of the vena contracta during the opening or closing process (see the bottom image of Figure 2). This shift of the vena contracta position can be prevented by designing a vertical flow direction in this area (see the middle image of Figure 2), which also enables a linear transfer function between the opening width s^* and the mass flow rate $\dot{m}$. This ensures a global linearity between actuator's position and mass flow rate.
- The radial position of the vena contracta r^* determines the required displacement of the actuator s^*, which in turn influences the actuator's precision requirements.

A design iteration process has taken place beginning with the preliminary design as described above, refining critical design areas as identified in the CFD analysis, using 3D-print process for rapid prototyping and testing the produced prototypes on the flow bench to first evaluate the static (various fixed positions excluding actuator's installation) flow performance of prototypes similar to one shown in Figure 1. In the following section the test bench setup and the methodology followed to analyze the data will be described.

4 TEST BENCH SETUP AND EXPERIMENTAL DATA ANALYSIS

4.1 Test Bench Setup:

To validate the theoretical principles, extensive tests were conducted on the THN flow test bench, equipped with various sensors to monitor thermodynamic variables and evaluate the dosing system's performance (Figure 3). The setup uses an electric radial blower to generate air mass flow by drawing air through the pipes, offering the advantage of setting test conditions independently of an internal combustion engine. Since the initial focus is on analyzing the flow behavior via the variable Venturi, excluding the ICE at this stage simplifies testing and conserves resources.

The mass flow is measured using two Bosch HFM5 MAF sensors, positioned upstream of the nozzle and at the blower inlet. This arrangement ensures accurate measurement and rules out potential leaks. Two type K thermocouples and an ambient temperature sensor complement the setup, with the thermocouples placed analogously to the MAF sensors to detect temperature changes and calculate air density.

Absolute pressure sensors with a 0–2 bar range, an accuracy of 0.5%, and a response time under 1 ms are used to measure the pressure loss across the throttle point dynamically and precisely. Additional sensors are installed in the vena contracta and between the fixed and movable parts, enabling analysis of actuator forces and thermodynamic conditions in these regions.

Central to the system are fast-response aerodynamic probes (FRAPs) from Vectoflow GmbH, which utilize piezoresistive pressure transducers to measure dynamic pressure within the pipe. [2], [13], [14]. The rake design, comprising five individual sensor heads, facilitates detailed pressure distribution analysis across the

pipe cross-section, enhancing the understanding of the flow profile. The flow bench is controlled via dSPACE rapid prototyping hardware, capable of recording FRAP data at frequencies up to 15 kHz. Post-processing of these high-frequency measurements is further detailed in the subsequent section. The central question is whether this sensing method will allow us to characterize the flow and extract the turbulence parameters in addition to timely resolve the actual mass flow rate under highly transient operating conditions.

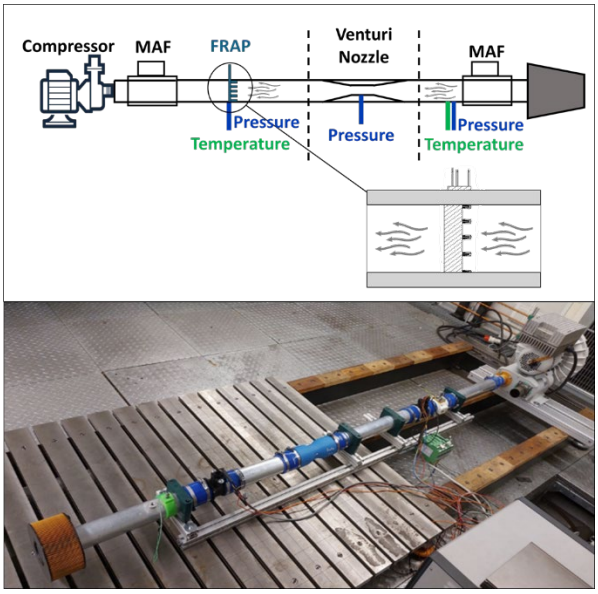

Figure 3. Top: Schematic representation of the flow bench setup including the position of the used sensors; Bottom: real installation in the lab of THN

4.2 High Frequency Data Post-Processing to extract flow and turbulence parameters

The FRAP signals were converted into a usable signal level (0–10 V) using measurement amplifiers based on the sensitivity specified by the manufacturer (Vectoflow GmbH). Subsequently, high-precision calibration data from Vectoflow were used to correct the individual probe heads (amplitude gain and phase shift). The raw signals are decomposed into a frequency spectrum using FFT to identify additional flow influences. The signal recorded by a FRAP corresponds to the difference between the stagnation pressure at the probe position p_t and the static pressure p at the outer wall of the pipe, as shown in the following equation.

$$p_t - p = \frac{1}{2}\rho u^2 \qquad (3)$$

This so-called dynamic pressure is then used to determine the velocity u at the lateral coordinate position of the probe. Since the flow belongs to the turbulent regime, the velocity signal consists, as described below, of a mean value and a fluctuation:

$$u = U + u' \qquad (4)$$

Using high-frequency measurement techniques, flow conditions can be resolved up to a frequency of 15 kHz. The recorded pitot pressures from the probes can be further analyzed using FFT analysis.

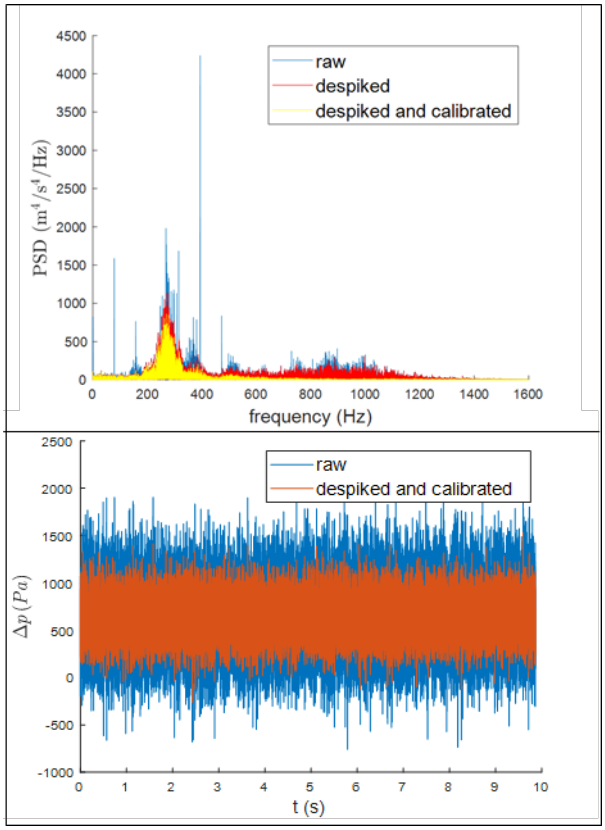

Figure 4. Top: power spectral density (PSD). Bottom: time domain transformation of despiked and calibrated signal (orange)

The mean value is required to obtain the average velocity profile across the pipe cross-section, which is used to estimate the mass flow rate. On the other hand, the statistics of velocity fluctuations provide insights into the transport and dissipation of turbulence. These quantities are characterized using turbulent scales. Since noise is unavoidable during experiments, the recorded fluctuations consist of statistical noise and physical fluctuations. The necessary cleaning of the recorded signals was performed in the frequency domain, obtained through a fast Fourier transform of the signals. The top image of Figure 4 shows in blue the power spectral density of the dynamic pressure fluctuations at an operating point. The sharp peaks occurring at regular intervals are attributed to the blower driving the flow. These peaks can be identified using an algorithm that employs the

median and the median absolute deviation [16]. Once the positions of the peaks are identified, the spectral power density values at these positions can be replaced by the mean of the surrounding values. The result is shown in red on the top image of Figure 4. By applying the calibration data provided by Vectoflow to the results, the measurements can be further corrected, represented by the yellow curve in the same figure. In the final step, before the frequency data is transformed back into time data, statistical noise is removed. The simplest method for this is spectral subtraction. This method assumes stationary additive noise, which affects the measurement at an operating point in the same way as it does during a baseline measurement. The baseline measurement corresponds to measuring the FRAP signals with the blower running but decoupled from the pipe system. In this condition, no flow occurs through the pipe system, and the probes record only ambient noise. The PSD of the noise is calculated and subtracted from the power density of the desired operating point. Transforming the results back into the time domain, as shown on the bottom of Figure 4, reveals that the applied corrections reduce the standard deviation of the raw signal, thus partially removing statistical noise while keeping physical fluctuations (red profile).

Before converting this dynamic pressure signal into a velocity signal, frequencies above 5 kHz are removed using a sixth-order Butterworth filter. The dynamic pressure values can now be converted into velocity and further analyzed. First, the autocorrelation of the fluctuations ρ is calculated by equation (5) and is shown on the top of Figure 5.

$$\rho_{ac}(\Delta x) = \frac{\overline{u'(x) \cdot u'(x+\Delta x)}}{\overline{u'^2}} \qquad (5)$$

Autocorrelation describes the similarity of a signal with a time-shifted copy of itself. This provides an estimate of the time over which fluctuations are correlated with themselves. Using the Taylor hypothesis of frozen turbulence, time-domain data can be converted into spatial data. Integrating the autocorrelation over all time or spatial shifts yields the integral time or length scale of the system (equation (6)):

$$L = \int_0^\infty \rho(\Delta x)\, d\Delta x \qquad (6)$$

Due to the fluctuations visible in the top image of Figure 5, it is common in the literature to define a threshold value for the autocorrelation, up to which the integration is performed. However, this introduces uncertainties, as the result is highly dependent on the chosen threshold. Alternatively, the analysis can be conducted in the frequency domain. After performing a fast Fourier transform, plotting the spectral power density of velocity fluctuations on a double logarithmic scale, as shown in the bottom image of Figure 5, reveals the spectrum of turbulent kinetic energy (TKE). The black line, delimited by the two vertical orange lines, represents the inertial subrange governed by the universal Kolmogorov −5/3 law. In this regime, turbulent energy is isotropically transferred from large to small scales. A least square fit of the universal law to the inertial subrange provides an estimation of the energy dissipation range which renders turbulent length scale. In this paper a different methodology is chosen however.

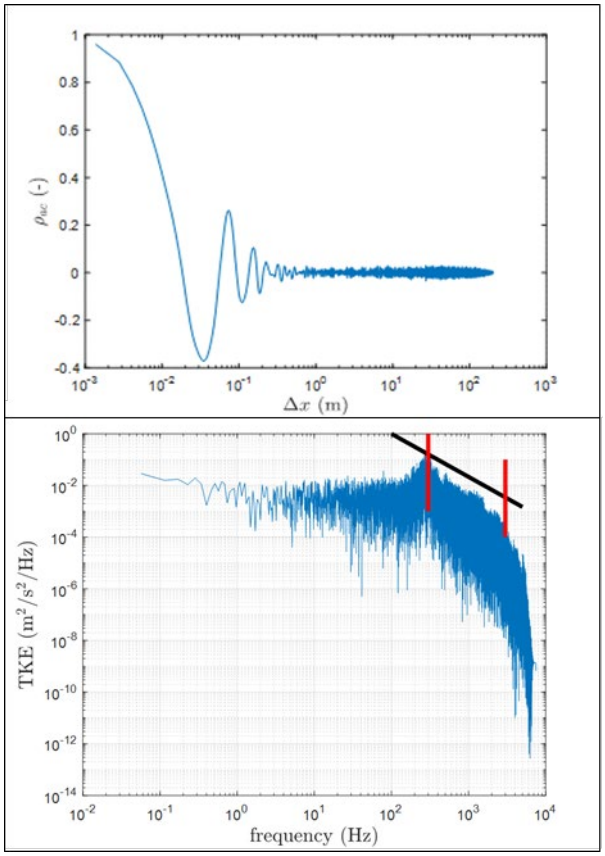

Figure 5. Top: autocorrelation of the velocity. Bottom: calculated turbulent kinetic energy spectrum; vertical bars represent the delimiters of the inertial range with a slope of -5/3 (black solid line)

A first order estimation of turbulence parameters, i.e. integral lengthscale and Kolmogorov scale, is provided by the analysis of zero crossings (ZC) of the turbulent velocity fluctuations. It was shown by Rice [15] that for a statistically stationary random process u, the average distance between (ZC) of the signal can be evaluated via the second order moments of the variable u and its derivative du/dx which both are assumed to have Gaussian

distributions. Several studies (e.g. Sreenivasan [17]) have shown that this method leads to a good estimation of the Taylor scale ($\lambda = \pi \cdot n_s^{-1}$, where n_s is the number density of ZC) even for non-Gaussian processes as usually encountered in turbulence. Using the relationship between the Taylor scale and the energy dissipation rate ϵ for isotropic turbulence ($\epsilon = 15\nu\frac{u'^2}{\lambda^2}$), a first estimate of the Kolmogorov scale $\eta = \left(\frac{\nu^3}{\epsilon}\right)^{1/4}$, can be provided. In literature several approaches for dealing with the upper bound of the integral in (6) can be found. In this paper a first estimate of L is obtained by integrating the autocorrelation function up to the first zero crossing. This approach was chosen to be consistent with the work of Mora et al. [18] In their paper, Mora et al. go on to propose an alternative method for estimating L via the statistics of the intervals ΔZ between two successive ZC based on the work of McFadden [19] and Smith et al. [24]. The integral lengthscale obtained by this method will be referred to as L_{McF} and is calculated via (7).

$$L_{McF} \approx \frac{\pi}{4}\frac{\mathrm{Var}(\Delta Z)}{\langle \Delta Z \rangle} \tag{7}$$

All measurements obtained are single point time measurements. The analysis conducted in the time domain can be easily translated to the spatial domain by application of Taylor's frozen turbulence hypothesis which relates time points t to spatial points

$$x = U \cdot t \tag{8}$$

where U is the mean convective velocity. Before evaluating the Taylor scale, one has to make sure that the number density n_s of zero crossings (ZC) is sufficiently resolved. In order to test this requirement, the fluctuating velocity signal is low-pass filtered at different scales and the corresponding number density is evaluated. For cutoff frequencies higher than a certain value f_c^* a plateau is reached and n_s is sufficiently resolved, see top and middle image of Figure 6.

The integral length scales obtained by both methods fairly agree and their ratio lies in the interval between numerical values of 0.88 and 1.04:

$$0.88 < \frac{L_{McF}}{L_{ac}} < 1.04 \tag{9}$$

The agreement between the results from these different methods proposes the usage of McFadden's theory for a first estimation of the integral lengthscale. This is advantageous in situations where an accurate estimation of the autocorrelation function is not possible. Apart from uncalibrated sensors, those include unexpected instationary noise in which more sophisticated denoising and despiking strategies are needed which nevertheless cannot guarantee robustness. Since the proposed method utilises statistics of zero crossings only, it is more robust against disturbances since it is not dependent on the amplitude of the fluctuations. The method also shows capability of capturing the trend of Reynolds dependency of the length scales between different operating points.

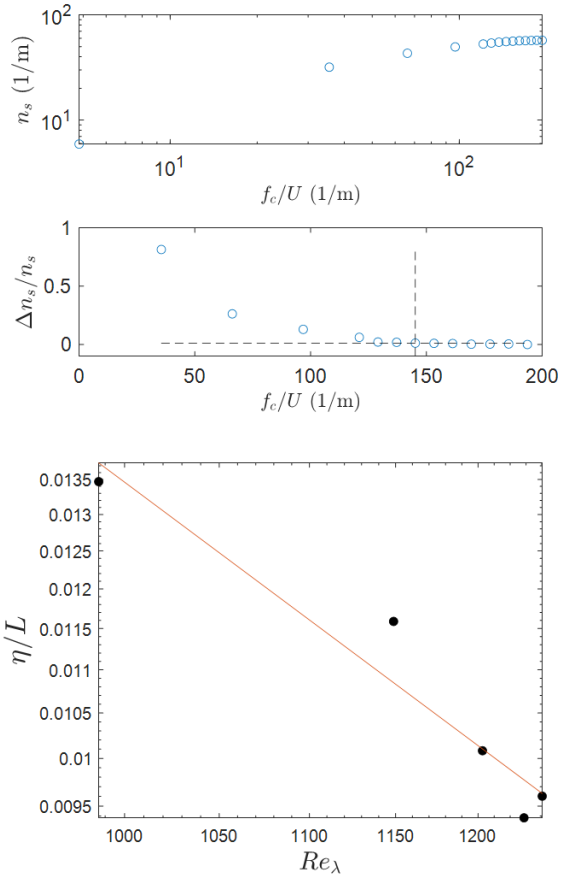

Figure 6. Top: Number Density of Zero Crossings (ZC) as a function of cut-off frequency. Bottom: Reynolds dependent ratio of turbulence scales

According to scaling arguments, see Pope [21], an exponential relation between the ratio of microscopic and macroscopic scales and the (Taylor-) based Reynolds number can be formulated, i.e.:

$$\frac{\eta}{L} \sim Re_\lambda^{-3/2} \tag{10}$$

A linear regression of the observed experimental points is depicted in the bottom image of Figure 6.

The linear regression provides a value of -1.55 for the exponent and a coefficient of determination of R^2= 0.93. In this section we demonstrated the ability of the FRAP's to resolve the turbulence parameters. Last but not least, it is worth mentioning that the measurement of the smallest turbulence scales requires that these scales are bigger than the resolution of the used equipment, which is ensured by the high frequency response of the used sensors.

5 COMPARISON OF TRANSIENT RESPONSE: VENTURI SYSTEM VS. THROTTLE BODY

The rapid changes in velocity that can be captured facilitates the high frequency resolution of the mass flow admitted through the system. This enables the accurate system identification of the Venturi system, which includes very small rise time, low overshoot and highly damped oscillations as demonstrated in Figure 7. It does not only help understanding the system at hand but is of great assistance in the Venturi development and design optimisation. For the reasons mentioned above the FRAP's are an excellent engine development tool.

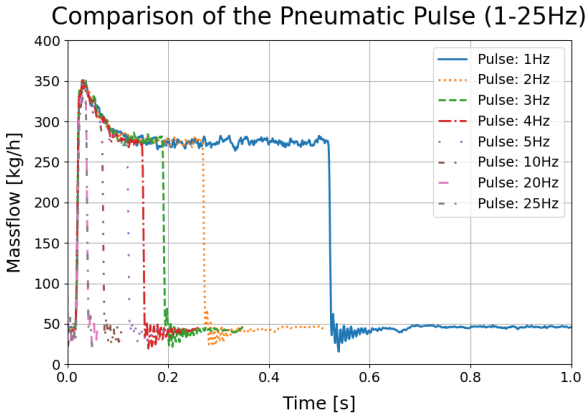

Figure 7 Measured dynamic response of the prototype Venturi System at various frequencies and 0 to 100% step load, simulating very fast transients between idle and full load engine operating conditions.

The top image of Figure 8 illustrates the dynamic response of the variable Venturi nozzle, actuated at a high frequency of 25 Hz. During testing, rapid transitions in mass flow were demanded between the fully closed and fully open positions, simulating the transient engine response from idle to full load conditions. The results demonstrate excellent repeatability and precise control of mass flow under these extreme transient conditions. However, with the current actuator setup, holding intermediate positions is not feasible, which limits the ability to perform smaller step responses within the mid-range between idle and full load conditions in the current test environment.

In contrast, the bottom image of Figure 8 presents the response of a throttle body, operating at a significantly lower frequency of 4 Hz (six times slower than the Venturi system). The data reveals bouncing at the fully closed position, resulting in inconsistent mass flow values during idle conditions, ranging between 10 and 225 kg/h. This indicates that the throttle body does not fully close at a frequency of 4 Hz. Additionally, at fully open positions, the mass flow varies from event to event, highlighting the limitations of throttle valves in controlling air mass flow under highly transient engine conditions.

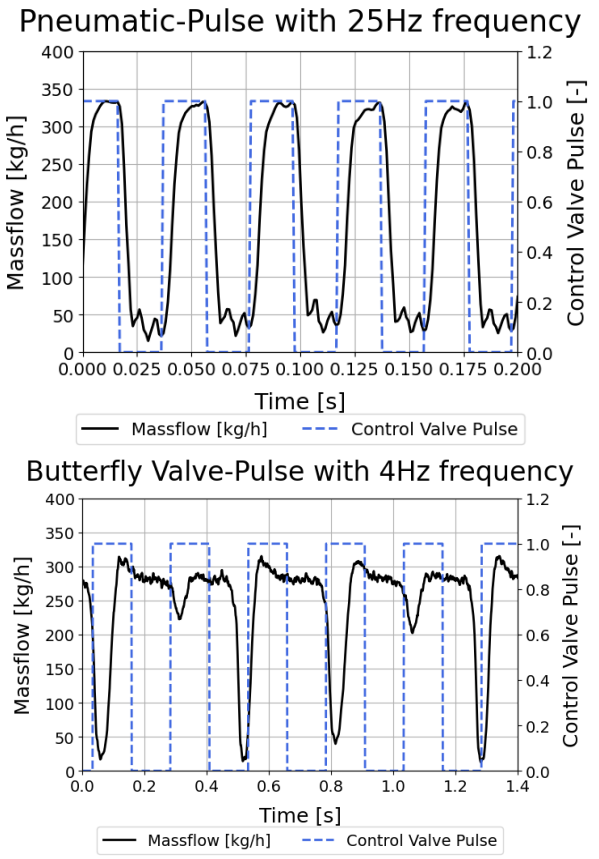

Figure 8. Top: measured dynamic response of air mass flow using the Venturi system at an actuation frequency of 25 Hz. Bottom: measured air mass flow showing the throttle body's response at an actuation frequency of 4 Hz.

Figure 8 emphasizes the dynamic capabilities of the variable Venturi nozzle, a critical component for achieving precise air mass flow control in aggressive transient scenarios. Transient conditions are particularly relevant in advanced powertrains, where engines frequently operate across a wide range of load conditions. The nozzle's ability to rapidly and reliably transition between fully closed and fully open states is

essential for maintaining optimal combustion conditions in terms of precise air-to-fuel ratio control, minimizing emissions, and improving system response time.

However, the inability to hold intermediate positions, which is caused by the current actuator design, restricts the system's capability to manage fine adjustments in air mass flow, which are often required during partial-load operation or in response to real-time driver inputs. Overcoming this limitation will involve integrating advanced actuators, such as stepper motors or piezoelectric systems, which offer higher precision and responsiveness. This improvement will enable the nozzle to adapt to a broader range of operating conditions, further enhancing its applicability in hybrid systems, fuel cells, and other advanced energy systems. Additionally, ongoing research into transient performance under varying environmental conditions (e.g., temperature and pressure) will refine its design for real-world applications.

6 EVALUATION OF CYCLE-RESOLVED AIR-FUEL RATIO CONTROL -IMPACT ON NO_X EMISSIONS

Transient dynamometers and engine test rigs have shown that during rapid acceleration or deceleration, λ can temporarily deviate from stoichiometric values due to time lags in air and fuel delivery systems. NOx emissions spike during these deviations, particularly under lean conditions. For example, real-world driving cycles (e.g., WLTP or FTP-75) reveal that NOx emissions are disproportionately high during transient phases compared to steady-state operation. Transient simulations using tools like GT-Power, or WAVE (by Realis software) confirm the observed trends. In the current study we are using WAVE to simulate the FTP-75 driving cycle. The air-fuel ratio (AFR) is defined by equation 11:

$$AFR = \lambda \times AFR_{stoich} \quad (11)$$

where AFR_{stoich} for hydrogen is approximately 34.2 kg air per kg hydrogen. The connection between transient λ deviations and NOx emissions is not a mere belief but a well-documented phenomenon underpinned by combustion science, empirical data, and validated simulation models. Recent studies analyzed the relationship between air-fuel ratio fluctuations and transient NOx emissions [22], [23]. They emphasize that deviations from the stoichiometric air-fuel ratio during rapid load transitions result in elevated NOx and hydrocarbon emissions. These deviations arise from incomplete combustion and suboptimal performance of the three-way catalytic converter. This phenomenon is particularly pronounced under transient conditions, such as load increase or throttle adjustments. The adopted methodology in the current study for simulating a transient driving cycle combines comprehensive modeling, real-world driving dynamics, and advanced simulation tools to evaluate the performance and emissions of an internal combustion engine under dynamic operating conditions. A detailed vehicle model has been developed in Simulink, allowing the integration of various subsystems and their dynamic interactions. Key parameters include:

- Vehicle mass (1150 kg) and engine mass (100 kg): These determine the overall inertia and load characteristics of the system.
- Axle inertia (2.592 kg·m²): Captures the rotational dynamics of the drivetrain.
- Transmission system: A six-speed manual gearbox is modeled, with gear ratios ranging from 3.55 (1st gear) to 0.69 (6th gear). Clutch inertia (0.01 kg·m²) and gearbox output shaft inertia (0.0591 kg·m²) are included for precise drivetrain representation.

This level of detail ensures that the vehicle's response to transient conditions such as acceleration, deceleration, and gear shifts can be accurately simulated.

To analyze air-to-fuel ratio variations during transient conditions, the WAVE software (by Realis) is employed. This one-dimensional gas exchange simulation tool enables cycle-resolved studies, incorporating:

- A steady-state validated model of a Euro 6-compliant inline three-cylinder turbocharged direct-injected gasoline engine. This serves as the foundation for transient simulations.
- Transient behavior analysis: Real-time changes in λ, influenced by the interplay between the throttle, fuel injection, and turbocharger, are captured. These dynamics are critical for emissions modeling.

The use of cycle-resolved air-fuel ratio spikes as an indicator of engine-out NOx emissions is a well-supported approach in engine modeling and emissions analysis, especially when assessing transient driving cycles like the FTP-75. This methodology is grounded in several experimental studies that show a strong correlation between transient λ-deviations and increased NOx emissions during dynamic driving conditions such as acceleration and deceleration [22], [23]. Another practical reason for employing this indirect method to evaluate transient NOx emissions is that emissions models used for transient driving cycle simulations often rely on simplified combustion

models, such as imposed heat release rates or Vibe functions. These models, being semi-empirical in nature, inherently introduce inaccuracies. Hence in author's opinion, the indirect method provides a more robust approach to capturing the dynamics of transient emissions behavior.

The results displayed in Figure 9, comparing the performance of the throttle body (represented by the dashed line) and the variable venturi (with a time constant of 50 ms, corresponding to 20 Hz, shown as the solid line), indicate a significant reduction in spikes when the variable venturi is incorporated into the engine's control system instead of the conventional throttle body. This is a promising outcome for further system development and testing under real engine conditions.

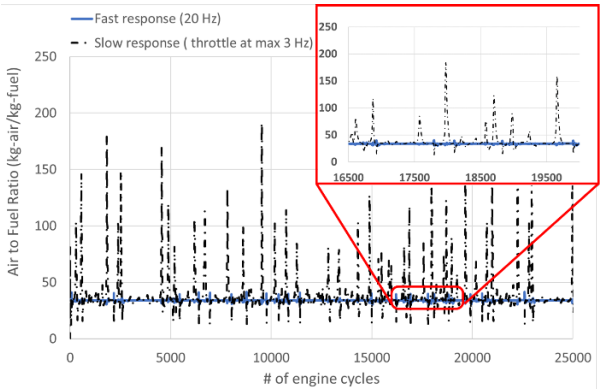

Figure 9. Air-fuel ratio (AFR) response during FTP-75 based on transient WAVE simulations. Black dotted line: cycle resolved AFR with conventional throttle body dynamics. Blue line: cycle resolved AFR with Venturi system.

The above described advantage of cutting the spikes of transient NOx emissions is further enhanced by the associated reduction in fuel consumption, as illustrated in Figure 10.

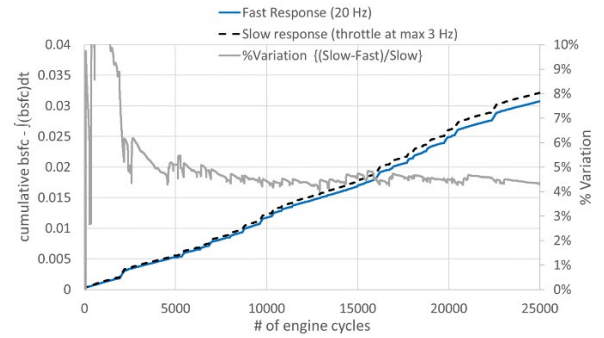

Figure 10. cumulative brake specific fuel consumption (bsfc) during FTP-75 based on transient WAVE simulations. Black dotted line: cycle resolved AFR with conventional throttle body dynamics. Blue line: cycle resolved AFR with Venturi system.

The cycle-specific brake specific fuel consumption (bsfc), integrated over the entire cycle, is represented on the left y-axis, offering a clear measure of the fuel efficiency improvements achieved. These gains are highlighted by the difference between the Venturi system and the throttle body, as shown by the grey curve on the right y-axis. A minimum fuel consumption benefit of 4% is demonstrated during the FTP-75 cycle, with even bigger improvements anticipated under more aggressive transient cycles. Moreover, the negative impact of over-lean (high AFR) or over-rich (low AFR) conditions, which adversely affect fuel consumption, is not accounted for in the combustion model utilized in the underlying transient WAVE simulation. This model is calibrated for stationary and stoichiometric operating conditions and, therefore, tends to overestimate the engine's efficiency when operating outside its calibrated range. This bias inadvertently favors the throttle body, suggesting that the actual performance benefits of the Venturi system compared to the throttle body are likely even greater than indicated by the simulation results.

7 CONCLUSIONS

This paper introduced a novel approach to overcoming the limitations of conventional throttle body systems by developing a device that operates an order of magnitude faster than a butterfly valve while minimizing flow losses. The design philosophy has been outlined, and the flow bench setup used to evaluate the performance of an instrumented prototype has been presented. High-frequency data collected during testing have been analyzed, and the extracted flow structure and turbulence parameters have been discussed.

The throttle body dynamics and Venturi-based system performance - validated through flow bench testing and incorporated into the WAVE transient model - provide the necessary accuracy to simulate the precise response of the cycle-resolved air-fuel ratio. The assessment of the emissions reduction strategy under transient conditions has been based on the device's ability to precisely manage AFR during each engine cycle, as derived from the transient model's output. The results have demonstrated that the new device outperforms the conventional butterfly valve in terms of responsiveness and emissions control.

By mitigating NOx spikes and reducing fuel consumption simultaneously, this approach underlines the importance of advanced control strategies and precise air-fuel metering in optimizing engine operation under certain conditions.

Future investigations will explore the broader implications of these findings, such as the scalability of this method to different engine sizes or types, and its integration into hybrid or alternative powertrain systems. Additionally, further validation under real-world driving cycles should be planed to provide valuable insights into the robustness and practicality of the proposed approach.

8 DEFINITIONS, ACRONYMS, ABBREVIATIONS

A^*	Cross-sectional area at the narrowest point (vena contracta)
AFR	Air-Fuel Ratio
ρ	Density
ρ_{ac}	Autocorrelation of the fluctuations
λ	Lambda value (air-fuel ratio indicator), Taylor Scale
κ	Adiabatic Exponent
η	Kolmogorov Scale
ε	Turbulent Energy Dissipation Rate
Δx	Time or spatial shift
ZC	Zero Crossings
WLTP	Worldwide Harmonised Light-Duty Vehicles Test Procedure
u'	Fluctuation of the flow velocity
u	Flow velocity
U	Mean flow velocity
TKE	Turbulent Kinetic Energy
THN	Technische Hochschule Nürnberg
s^*	Opening width of the Venturi system
Re_λ	Reynolds number based on Taylor scale
Re_λ	Radial position of the vena contracta
p_t	Total Pressure (static + dynamic pressure)
PSD	Power Spectral Density
p	Pressure
NOx	Nitrogen Oxides
MAF	Mass Air Flow Sensor
M(x)	Mach number distribution
m	Mass Flow Rate
L	Integral Length Scale
ICE	Internal Combustion Engine
H_2-ICE	Hydrogen Internal Combustion Engine
bsfc	Brake specific fuel consumption
FTP-75	Federal Test Procedure
FRAP	Fast-Response Aerodynamic Probe
FFT	Fast-Fourier Transformation
ECU	Engine Control Unit
CFD	Cumputational Fluid Dynamics
CAD	Computer-Aided Design

9 ACKNOWLEDGMENTS

This work was supported by the Deutsche Forschungsgemeinschaft (DFG, German Research Foundation) Project-ID 528480942 - FIP 8 and the Bavarian Ministry of Economic Affairs, Regional Development and Energy, 41-6562b/37/2-VAL-2209-0008, V2-DoRR – Variable Venturi Nozzle for precise dosing of Reactants in Hydrogen Propulsion Systems for Ultimate Control Accuracy under Highly Dynamic Operating Conditions

10 REFERENCES AND BIBLIOGRAPHY

[1] R. Hu, F. Zhang, Z. Peng, and Y. Pei, “The NOx emission characteristics of gasoline vehicles during transient driving cycles,” *Transportation Research Part D: Transport and Environment*, vol. 109, p. 103386, Aug. 2022, doi: 10.1016/j.trd.2022.103386.

[2] F. Großmann, T. Mühlpfordt, P. Rambacher, and G. Bikas, “Crank-Angle Resolved Flow Measurements in the Intake Duct of a Research Engine Using Novel and Fast Response Aerodynamic Probes,” *Front. Mech. Eng.*, vol. 7, p. 633690, Feb. 2021, doi: 10.3389/fmech.2021.633690.

[3] F. Ozkan, M. Ozturk, and A. Baylar, “Experimental investigations of air and liquid injection by venturi tubes,” *Water & Environment J*, vol. 20, no. 3, pp. 114–122, Sep. 2006, doi: 10.1111/j.1747-6593.2005.00003.x.

[4] H. O’Hern, T. Murphy, X. Zhang, J. Liburdy, and B. Abbasi, “A Design Method for Low-Pressure Venturi Nozzles,” *Applied Mechanics*, vol. 3, no. 2, pp. 390–411, Apr. 2022, doi: 10.3390/applmech3020024.

[5] A. Petrovic, J. Svorcan, A. Pejcev, D. Radenkovic, and A. Petrovic, “Comparison of novel variable area convergent-divergent nozzle performances obtained by analytic, computational and experimental methods,” *Applied Mathematical Modelling*, vol. 57, pp. 206–225, May 2018, doi: 10.1016/j.apm.2018.01.016.

[6] V. Van Nguyen, S. Varga, J. Soares, V. Dvorak, and A. C. Oliveira, "Applying a variable geometry ejector in a solar ejector refrigeration system," *International Journal of Refrigeration*, vol. 113, pp. 187–195, May 2020, doi: 10.1016/j.ijrefrig.2020.01.018.

[7] F. Liu, E. A. Groll, and D. Li, "Investigation on performance of variable geometry ejectors for CO 2 refrigeration cycles," *Energy*, vol. 45, no. 1, pp. 829–839, Sep. 2012, doi: 10.1016/j.energy.2012.07.008.

[8] K. Kodo, "Variable venturi type carburetor," JPS58128454A, Jun. 19, 1987

[9] W. P. Patterson and R. J. Bailey, "High energy emulsifier," WO1983001210A1, Apr. 14, 1983

[10] Renault SAS, "Variable floe elastic nozzle," FR2326235A1, Apr. 20, 1979

[11] G. Bikas, R. Falgenhauer, and P. Weigand, "Control of a flow of a fluid into a reaction chamber of an thermo-chemical or electro-chemical energy conversion machine," EP4183479A1, May 24, 2023

[12] J. Spurk and N. Aksel, *Strömungslehre: Einführung in die Theorie der Strömungen*. Berlin, Heidelberg: Springer Berlin Heidelberg, 2019. doi: 10.1007/978-3-662-58764-5.

[13] F. M. Heckmeier, D. Iglesias, S. Kienitz, and C. Breitsamter, "An Innovative Development of a Five-Hole Pressure Probe for Highly Unsteady Flow Phenomena," in *Volume 6: Ceramics; Controls, Diagnostics, and Instrumentation; Education; Manufacturing Materials and Metallurgy*, Phoenix, Arizona, USA: American Society of Mechanical Engineers, Jun. 2019, p. V006T05A001. doi: 10.1115/GT2019-90079.

[14] F. M. Heckmeier, S. Hayböck, and C. Breitsamter, "Spatial and temporal resolution of a fast-response aerodynamic pressure probe in grid-generated turbulence," *Exp Fluids*, vol. 62, no. 2, p. 44, Feb. 2021, doi: 10.1007/s00348-021-03141-7.

[15] S. O. Rice, "Mathematical Analysis of Random Noise," *Bell System Technical Journal*, vol. 24, no. 1, pp. 46–156, Jan. 1945, doi: 10.1002/j.1538-7305.1945.tb00453.x.

[16] D. A. Whitaker and K. Hayes, "A simple algorithm for despiking Raman spectra," *Chemometrics and Intelligent Laboratory Systems*, vol. 179, pp. 82–84, Aug. 2018, doi: 10.1016/j.chemolab.2018.06.009.

[17] K. R. Sreenivasan, A. Prabhu, and R. Narasimha, "Zero-crossings in turbulent signals," *J. Fluid Mech.*, vol. 137, pp. 251–272, Dec. 1983, doi: 10.1017/S0022112083002396.

[18] D. O. Mora and M. Obligado, "Estimating the integral length scale on turbulent flows from the zero crossings of the longitudinal velocity fluctuation," 2020, *arXiv*. doi: 10.48550/ARXIV.2005.06055.

[19] J. McFadden, "The axis-crossing intervals of random functions--II," *IEEE Trans. Inform. Theory*, vol. 4, no. 1, pp. 14–24, Mar. 1958, doi: 10.1109/TIT.1958.1057438.

[20] N. Mazellier and J. C. Vassilicos, "The turbulence dissipation constant is not universal because of its universal dependence on large-scale flow topology," *Physics of Fluids*, vol. 20, no. 1, p. 015101, Jan. 2008, doi: 10.1063/1.2832778.

[21] S. B. Pope, *Turbulent Flows*, 1st ed. Cambridge University Press, 2000. doi: 10.1017/CBO9780511840531.

[22] D. Lou, Y. Ren, X. Li, Y. Zhang, and X. Sun, "Effect of Operating Conditions and TWC Parameters on Emissions Characteristics of a Stoichiometric Natural Gas Engine," *Energies*, vol. 13, no. 18, p. 4905, Sep. 2020, doi: 10.3390/en13184905.

[23] Q. Liu, Z. Liu, Y. Han, J. Tian, J. Wang, and J. Fang, "Experimental Investigation of the Loading Strategy of an Automotive Diesel Engine under Transient Operation Conditions," *Energies*, vol. 11, no. 5, p. 1293, May 2018, doi: 10.3390/en11051293.

[24] J. M. Smith, K. I. Hopcraft, und E. Jakeman, „Fluctuations in the zeros of differentiable Gaussian processes", Phys. Rev. E, Bd. 77, Nr. 3, S. 031112, March 2008, doi: 10.1103/PhysRevE.77.031112.

11 CONTACT

For more information please contact:

Prof. Dr.-Ing. Georgios Bikas

Professor at Mechanical Engineering Department of Technische Hochschule Nuremberg, Ohm.

Kesslerplatz 12

D-90489 Nuremberg, Germany

Email: georgios.bikas@th-nuernberg.de

Phone: +49 911 5880 1711